Title

Polymorphic Variants of Human Protein l-Isoaspartyl Methyltransferase Affect Catalytic Activity, Aggregation, and Thermal Stability

Journal

Journal of Biological Chemistry, 292(9)

ISSN

0021-9258

Authors

Juang, Charity
Chen, Baihe
Bru, Jean-Louis
et al.

Publication Date

2017-03-01

DOI

10.1074/jbc.m116.765222

Peer reviewed

THE JOURNAL OF BIOLOGICAL CHEMISTRY VOL. 292, NO. 9, pp. 3656–3665, March 3, 2017

Polymorphic Variants of Human Protein L-Isoaspartyl Methyltransferase Affect Catalytic Activity, Aggregation, and Thermal Stability

*IMPLICATIONS FOR THE ETIOLOGY OF NEUROLOGICAL DISORDERS AND COGNITIVE AGING**

Received for publication, October 28, 2016, and in revised form, January 16, 2017 Published, JBC Papers in Press, January 18, 2017, DOI 10.1074/jbc.M116.765222

Charity Juang, Baihe Chen, Jean-Louis Bru, Katherine Nguyen, Eric Huynh, Mahsa Momen, Jeungjin Kim, and Dana W. Aswad[1]

From the Department of Molecular Biology and Biochemistry, University of California Irvine, Irvine, California 92697-3900

Edited by F. Anne Stephenson

Protein L-isoaspartyl methyltransferase (PIMT/PCMT1), a product of the human *pcmt1* gene, catalyzes repair of abnormal L-isoaspartyl linkages in age-damaged proteins. Pcmt1 knockout mice exhibit a profound neuropathology and die 30–60 days postnatal from an epileptic seizure. Here we express 15 reported variants of human PIMT and characterize them with regard to their enzymatic activity, thermal stability, and propensity to aggregation. One mutation, R36C, renders PIMT completely inactive, whereas two others, A7P and I58V, exhibit activity that is 80–100% higher than wild type. G175R is highly prone to aggregation and has greatly reduced activity. R17S and R17H show markedly enhanced sensitivity to thermal denaturation. Based on previous studies of moderate PIMT variation in humans and mice, we predict that heterozygosity for R36C, G175R, R17S, and R17H will prove detrimental to cognitive function and successful aging, whereas homozygosity (if it ever occurs) will lead to severe neurological problems in the young.

Protein L-isoaspartyl methyltransferase (PIMT/PCMT1; product of the *pcmt1* gene)[2] functions to repair abnormal isoaspartyl (isoAsp) sites in proteins that occur via isomerization of the peptide bond linking asparagine or aspartate residues to their carboxyl-flanking neighbor (1–3). isoAsp formation, like oxidation, is an extremely common type of spontaneous protein damage that occurs under mild conditions *in vivo* and *in vitro* and is known to alter protein function and antigenicity. PIMT utilizes the cofactor *S*-adenosyl-L-methionine (AdoMet) to transfer a methyl group onto the α-carboxyl group of isoAsp sites leading to a succinimidyl intermediate that subsequently hydrolyzes to L-Asp and L-isoAsp (Fig. 1). Continuing cycles of PIMT action efficiently repair L-isoAsp sites *in vitro* (4–9), and reduction of PIMT activity in cultured cells or KO mice dramatically increases the level of isoAsp-containing proteins (10–13). PIMT is widely distributed in mammalian tissues but is particularly rich in the CNS (14–17). A critical need for PIMT in brain is evident from the overt neurological phenotype of PIMT-deficient mice; increased brain size, abnormal neuroanatomical and electrophysiological properties of hippocampal cells along with reduced cognitive function (18), atypical open field behavior (19), and fatal epileptic seizures beginning at 4 weeks of age (11, 12). A proteomic study utilizing the PIMT-KO mouse revealed over 30 neuronal targets for PIMT, including synapsins I and II, CRMP2 (collapsin response mediator protein 2), dynamin 1, α- and β-tubulin, and creatine kinase B, among others (20). Based on the phenotype of the PIMT-KO mouse, a major reduction of PIMT repair activity in humans would likely contribute to neurodevelopmental disorders, including epilepsy, in the young. Moreover, current evidence suggests that even moderate decrements in PIMT activity accelerate age-related changes in cognition and even lifespan. Brain extracts of PIMT +/− mice have 50–55% of the PIMT activity found in WT (+/+) mice. Between 8 months and 2 years, male +/− mice accumulate six times more isoaspartyl damage than +/+ males (21) and have a median lifespan that is ~6 weeks shorter (22). Interestingly, female +/− mice accumulate approximately three times more isoaspartyl damage over the same time period but show no apparent reduction in lifespan. In WT mice, PIMT activity shows a modest decrease over the lifespan (21), but in postmortem human brain samples, the highest PIMT activities are found in the eldest (23). This latter observation suggests that a higher inherited PIMT activity in humans may promote longevity.

There is one polymorphism, at position 119 in human PIMT, in which both alleles (Val and Ile) are very common (see Table 1). Using erythrocyte cell extracts from humans of known genotype, it was previously found that PIMT activity is slightly higher and more thermally stable in Ile/Ile than Val/Val individuals, with heterozygotes exhibiting an intermediate level of activity and stability (24, 25). In contrast, extracts from Val/Val individuals were superior in binding isoaspartyl-damaged pro-

* This work was supported by private donations to the Department of Molecular Biology at the University of California Irvine; by funds from the Faculty Research and Travel Committee in the School of Biological Sciences of the University of California Irvine; and by a Summer Undergraduate Research Opportunity Award (to J.-L. B.). The authors declare that they have no conflicts of interest with the contents of this article.

[1] To whom correspondence should be addressed: Dept. of Molecular Biology and Biochemistry, 3205 McGaugh Hall, University of California Irvine, Irvine, CA 92697-3900. Tel.: 949-824-6866; E-mail: dwaswad@uci.edu.

[2] The abbreviations used are: PIMT or PCMT1, protein L-isoaspartyl methyltransferase, also known as protein carboxyl methytransferase type 1; AdoMet, *S*-adenosyl-L-methionine; isoAsp, isoaspartate or isoaspartyl; DSF, differential scanning fluorimetry, TMB, 3,3′,5,5′-tetramethylbenzidine.

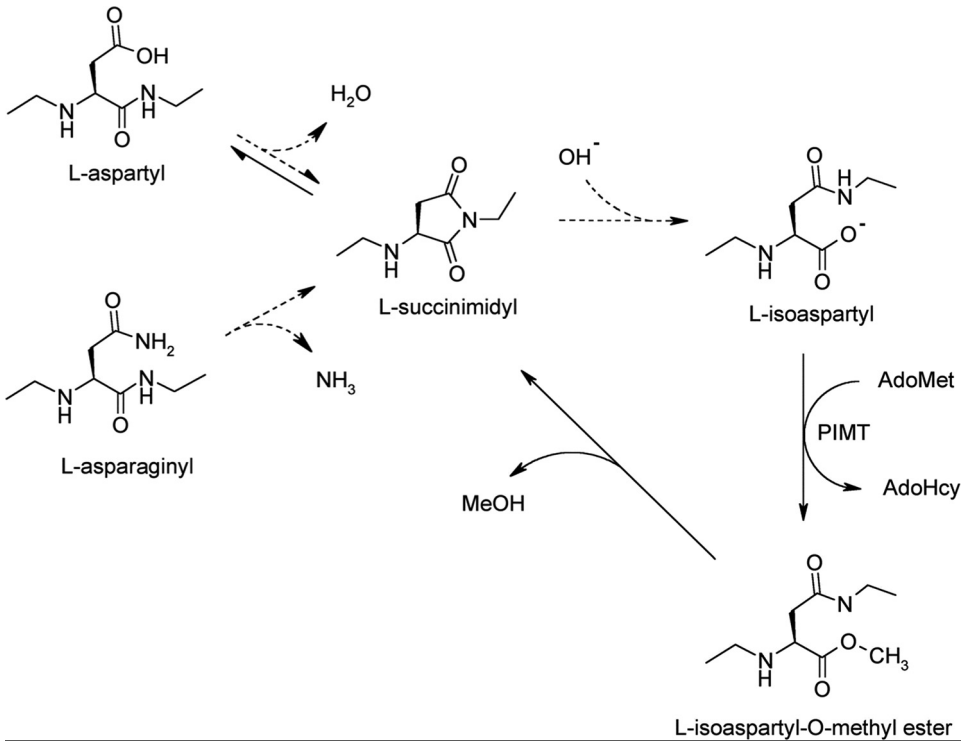

FIGURE 1. **Mechanism of isoaspartyl protein damage and PIMT-catalyzed repair.** Under physiological conditions, deamidation of asparagine residues or dehydration of aspartic acid residues results in the formation of a metastable intermediate succinimide that spontaneously hydrolyzes to form a mixture of normal L-aspartyl and atypical L-isoaspartyl linkages. PIMT, using AdoMet as a methyl donor, selectively methylates the isoaspartyl α-carboxyl group to form a highly labile methyl ester. Spontaneous demethylation occurs within minutes to reform the original succinimide, with release of methanol as a by-product. This succinimide is now the starting point for further cycles of repair, resulting in nearly complete conversion of the isoaspartyl β-linkages to normal aspartyl α-linkages. *Dashed arrows* indicate the damage reactions, and *solid lines* indicate the repair pathway.

teins obtained from PIMT-KO mouse brain, as indicated by a 30% lower K_m value in the methylation kinetics (25). This latter study also presented intriguing evidence for Val/Ile hybrid vigor at position 119. By comparing PIMT genotypes in populations of younger *versus* healthy older Ashkenazi Jews, it was found that the frequency of Val/Ile heterozygotes in the healthy older population (mean age, 87) was significantly higher ($p = 0.049$) than predicted by Hardy-Weinberg equilibrium. It thus appears that even modest changes in the profile of PIMT activity can have profound implications for human health.

Ongoing genome-wide association studies are generating massive amounts of data that are progressively uncovering the molecular basis of various diseases. Non-synonymous SNPs in protein coding regions account for a substantial fraction of all disease-related genetic mutations. Knowing how a given SNP actually affects the function of the protein in which it resides is an invaluable complement to such studies. For these reasons, we decided to express and purify known polymorphic variants of human PIMT and then characterize them with regard to their catalytic activity and thermal stability. Although it was not an original goal of this study, the findings reported here also provide some insight on the propensity of these variants for spontaneous aggregation, a characteristic that is also likely to affect PIMT activity *in vivo*.

Results

Expression and Aggregation of PIMT Variants—As of July 2015, the NCBI SNP database (dbSNP) contained 14 non-synonymous variants in the coding regions of the human *pcmt1* gene (Table 1). The minor allele frequency data in Table 1 was updated as of December 15, 2016.

As described under "Experimental Procedures," we used standard protocols to express and purify WT PIMT and all 14 of these variants. When subjected to SDS-PAGE, all of the purified enzymes exhibited a major band near the expected mass (28–30 kDa), but a pair of lighter bands was also evident at 65–70 kDa (Fig. 2). These higher mass bands were barely detectable for the WT and many of the mutants but very strong for G175R and moderately strong for several others. For those mutants that showed a relatively high level of high mass doublet, the relative abundance of these bands varied somewhat from prep to prep (Fig. 3*A*). We postulated that these bands could be due to 1) incomplete reduction of disulfide bonds during sample preparation for SDS-PAGE; 2) the formation of highly stable aggregates of PIMT during expression, purification, or storage; or 3) the presence of *Escherichia coli* proteins caused by incomplete purification. The results shown in Fig. 3*B* argue against incomplete disulfide reduction as a source of high mass bands. A 3-fold increase in DTT concentration during heating in sample buffer had no discernable effect on the staining patterns of either WT PIMT or the mutants with prominent high mass bands.

To test the "stable aggregates" hypothesis, we subjected WT and selected mutant PIMTs to Western blotting using an anti-T7 antibody (Fig. 4*A*). A T7 antigen sequence is located

TABLE 1

Non-synonymous SNPs in the coding region of the *pmct1* gene listed in the dbSNP as of July 2015

The amino acid positions in all the SNP databases are off by +59 because they assume an unused start codon upstream of the real start. Note that the status of these data was updated in the dbSNP in December 2016.

SNP ID	Variant	Count[a]	Alleles[b]	MAF[c]	Validation[d]	Source
				%		
rs11540603	A1V	1			Yes	dbSNP
rs200097071	A7P	23	119,506	0.019245	Yes	dbSNP
rs11540597	R17S	—[e]	—	—	Deleted	dbSNP
rs11540600	R17H	—	—	—	Deleted	dbSNP
rs11540602	A33S					dbSNP
rs374534669	R36C	2	13,006	0.015377	Yes	GO-ESP
rs11540596	H38N					dbSNP
rs143477308	I58V	1	13,006	0.007688		GO-ESP
rs148018752	F72L	56	121,122	0.046225	Yes	ExAC
rs186472718	A79G	1	5008	0.019968	Yes	1000G
rs4816	V119I	59,561	121,260	49.118758	Yes	ExAC
rs200029629	K124R	47	121,064	0.038834	Yes	ExAC
rs370117092	P162S	1	121,400	0.000822	Yes	ExAC
rs376806476	G175R	6	121,400	0.004943	Yes	ExAC

[a] Number of times the minor allele was found.
[b] Total number of alleles sequenced (twice the number of individuals sampled).
[c] Minor allele frequency, as a percentage of the total.
[d] Validation as designated in dbSNP. R17S and R17H were deleted on June 27, 2016 because of mapping or clustering errors.
[e] Dashes indicate no information provided in dbSNP. A7P data was not found in ExAC, but dbSNP cites ExAC as the source.

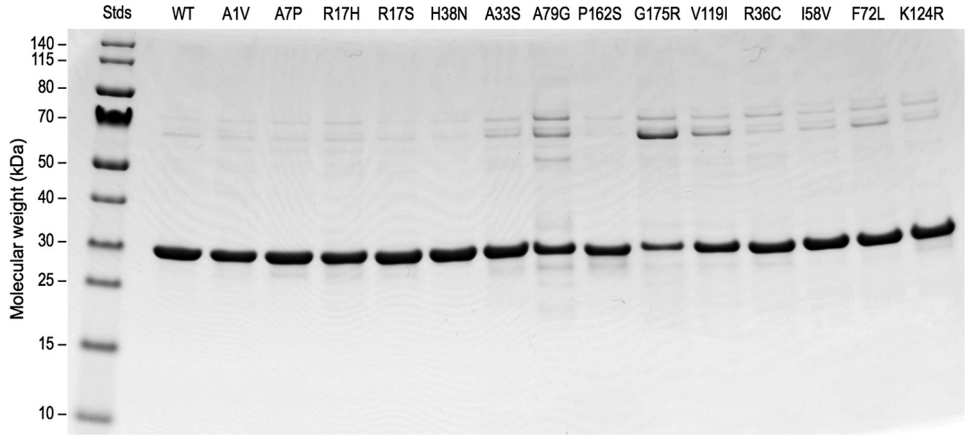

FIGURE 2. **SDS-PAGE of the 15 purified recombinant PIMT variants used in this study.** Each lane was loaded with 5 μg of protein. Electrophoresis and protein staining were carried as described under "Experimental Procedures." Bands suggesting the existence of stable PIMT aggregates are seen to varying degrees in all lanes but are most prominent with A79G, G175R, V119I, and F72L.

between the His tag and the N terminus of expressed proteins with our plasmid and serves as a useful mark to monitor expression. The results show clear evidence of putative dimer and higher mass aggregates for all samples on the gel, with WT PIMT showing the lowest level. The possibility that the T7 antibody reacts with certain endogenous *E. coli* proteins was considered, but this was ruled out by the results shown in Fig. 4*B* where a T7 blot was carried out on crude extracts from *E. coli* hosting an expression plasmid for the R17H PIMT variant. A strong T7 signal that correlates with R17H expression is seen at 29 kDa, but there is no discernable binding of the T7 antibody to any endogenous *E. coli* protein.

We conclude here that some SNPs of human PIMT, as exemplified best by G175R, are highly prone to spontaneous aggregation. The prominent bands at 60–65 kDa suggest the presence of PIMT dimers, and the stability of the aggregates suggests they arise either from non-reducible covalent cross-linking or highly stable non-covalent interactions akin to those associated with proteins such as β-amyloid and synuclein.

Enzymatic Activity of PIMT Variants—The methyltransferase activity of the WT human PIMT produced in this study was essentially identical to two previous reports from our lab wherein we expressed and purified recombinant PIMT starting from rat cDNA. The recombinant rat PIMT characterized by David and Aswad (26) was expressed without any tags and had a specific activity of 16.8 nmol/min of methyl transfer per mg of enzyme using the assay originally described by Aswad and Deight (27). The rat PIMT used by Zhu *et al.* (20) was expressed with a His/T7 tag (using the same plasmid as in the present study) and had a specific activity of 12.6–16.3 nmol/min of methyl transfer per mg of enzyme. The specific activity of our human WT PIMT is the same as that reported by Zhu *et al.*, and the activity remained within this range after complete removal of the His tag by thrombin cleavage (Fig. 5). Because the His/T7 tag does not affect WT PIMT activity, all of our activity and stability data were obtained with the N-terminal tags intact.

We used the methyltransferase assay detailed under "Experimental Procedures" to compare the activity of the 14 variants to WT PIMT (Fig. 6*A*). Except for position 119 in the PIMT sequence, all the variants are quite rare. The NCBI database considers valine at position 119 to be the WT, so this form was used as the basis of comparison in our study. Activity of three

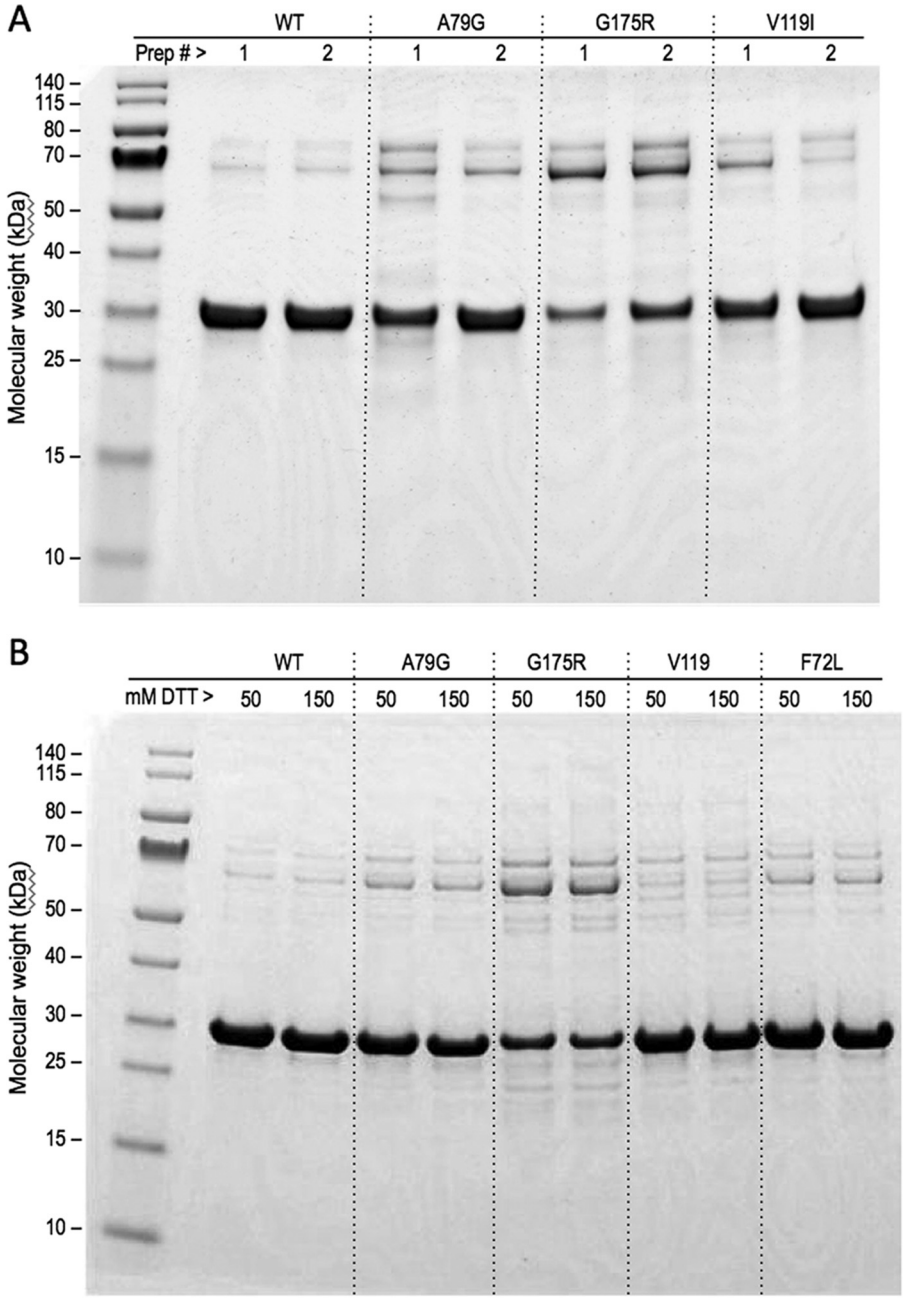

FIGURE 3. **The presence of high mass protein bands in certain mutants varies between expression preps and is not due to insufficient reduction of disulfide bonds prior to electrophoresis.** *A*, demonstration of moderate prep to prep variation in the staining pattern of WT PIMT and three mutants whose preparations show relatively high levels of putative aggregation. *B*, demonstration that the level of putative aggregates is not altered by more aggressive sample preparation prior to SDS-PAGE. The first lane in each pair was loaded with 5 μg of protein prepared according to our standard procedure (see "Experimental Procedures"), which involves heating for 10 min at 70 °C in sample buffer containing 50 mM DTT. In the second lane of each pair, heating was carried out for 5 min at 95 °C with 150 mM DTT.

variants is quite remarkable. R36C exhibits no detectable activity, whereas A7P and I58V have activity that is 80–100% higher than that of WT. Activity is reduced in G175R and F72L by ~40 and 20%, respectively.

The activity loss in G175R is likely related to its marked state of aggregation (Figs. 2–4). However, as explained under "Experimental Procedures," the specific activity data in Fig. 6 was normalized to the relative amount of protein that runs at 28 kDa, not the total amount of protein in the enzyme assay. Had we used total protein in the specific activity calculations, the activity of G175R would be only 20% of the WT.

Thermal Stability—Previous studies with human RBC extracts from genotyped individuals have shown a marked difference in thermal stability between the two common variants (Val *versus* Ile) in position 119 of PIMT. David *et al.* (24) found that preheating for 15 min at 52 °C resulted in activity losses of 80 and 20%, respectively. In a subsequent study with a different subject population, DeVry and Clarke (25) obtained qualitatively similar results. Fig. 6*B* shows the relative heat stability of our PIMT variants as judged by the ratio of activity in preheated (15 min at 52 °C) *versus* control (unheated) samples for each mutant. The *horizontal solid line* indicates the heated/control

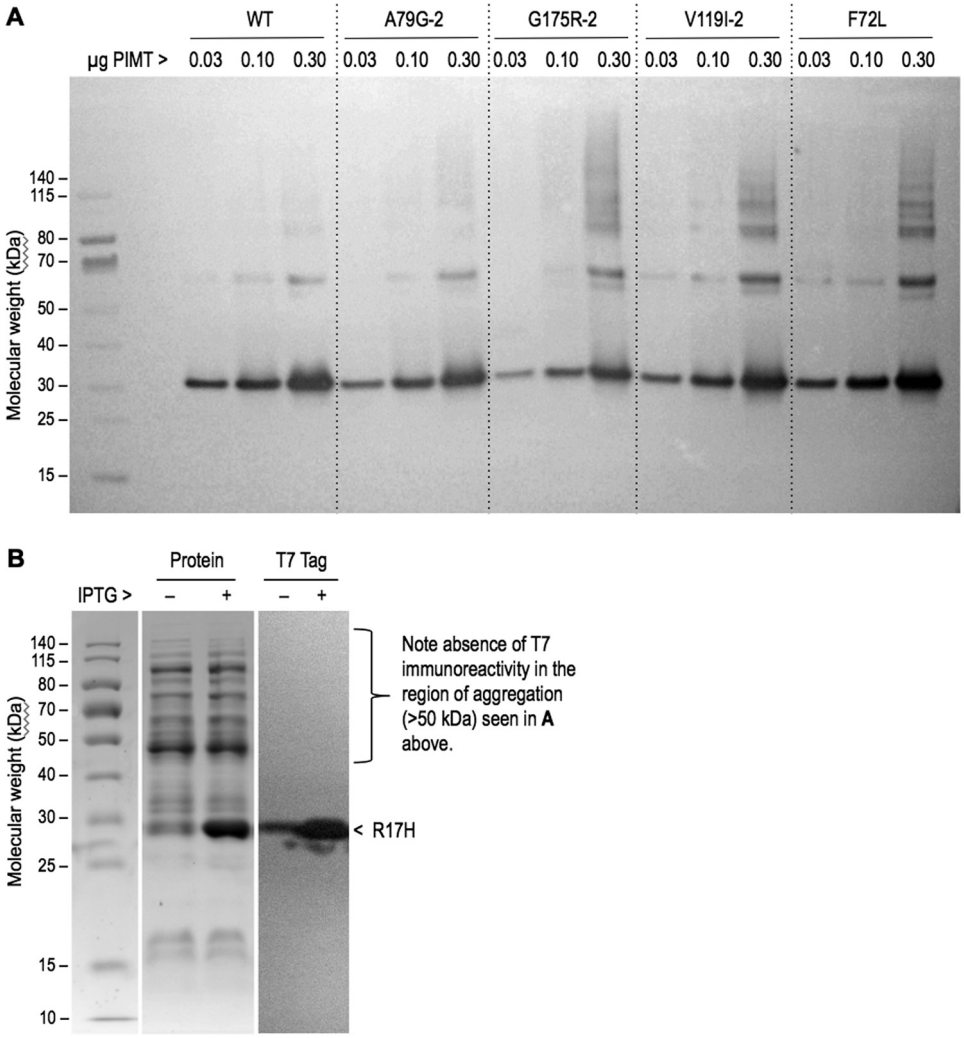

FIGURE 4. **Evidence that the high mass protein bands seen in Figs. 2 and 3 are stable aggregates of PIMT and not contaminants from the *E. coli* host.** *A*, Western blot of purified WT PIMT and three mutants. The blot was incubated with a 1:1000 dilution of HRP-conjugated rabbit anti-T7 tag antibody and then stained with TMB to selectively reveal the presence of recombinant protein. The pattern of immunostaining suggests the presence of a PIMT dimer at ~65 kDa, along with numerous aggregates of higher mass. *B*, the anti-T7 antibody does not react with *E. coli* host protein. The *middle panel* shows Coomassie staining of a gel comparing crude lysates of *E. coli* transformed with plasmid for PIMT mutant R17H, before (−) and after (+) induction by isopropyl β-D-thiogalactopyranoside (*IPTG*). The *right panel* shows a Western blot of the same extracts with immunostaining for the T7 tag, demonstrating that the anti-T7 antibody does not exhibit unexpected binding to *E. coli* host proteins in the lysates. The *left panel* shows molecular weight markers.

ratio obtained with WT PIMT (0.91), whereas the *dashed lines* indicate two standard deviations of this ratio. Four of the mutants (R17H, R17S, A33S, and G175R) exhibited a loss of activity that was well below the range seen for the WT. It is interesting that, with the exception of G175R, these mutants had basal specific activities (Fig. 6*A*) nearly identical to that of the WT.

We were surprised to see that neither the WT (Val-119) nor the Ile-119 variant lost much activity upon heating under these conditions. This prompted us to reinvestigate the thermal stability of all our PIMT variants by differential scanning fluorimetry (DSF). This method uses real time quantitative PCR instrumentation to obtain precise melting temperatures (T_m) via increased binding of a soluble fluorophor as a protein unfolds and exposes hydrophobic regions that are normally buried in the native protein (28). Our DSF results (Fig. 7) indicate that only 3 of the 14 variants (F72L, P162S, and K124R) have T_m values similar to the WT. Ile-119 has a T_m that is 1.6 °C higher, whereas all the remaining variants have significantly lower T_m values. The Ile-119 result is consistent with its enhanced thermal stability as observed in the two human RBC extract studies mentioned above. R17H and R17S have by far the lowest T_m values, consistent with our activity data in Fig. 6*B*. We were unable to determine a T_m for G175R because the DSF curve was highly abnormal. This is no doubt due to its high state of pre-existing aggregation.

Discussion

Aggregation—Among the 14 SNPs in this study, we found several that differ significantly from the WT with respect to aggregation, enzymatic activity, and thermal stability. All variants of PIMT exhibited a pair of bands in the 65–70-kDa region, but these were barely detectable for the WT and six of the mutants. Aggregation was most prominent for G175R, accounting for ~50% of the total protein. Based on molecular weight, it is likely that one or both of the 65–70-kDa bands are

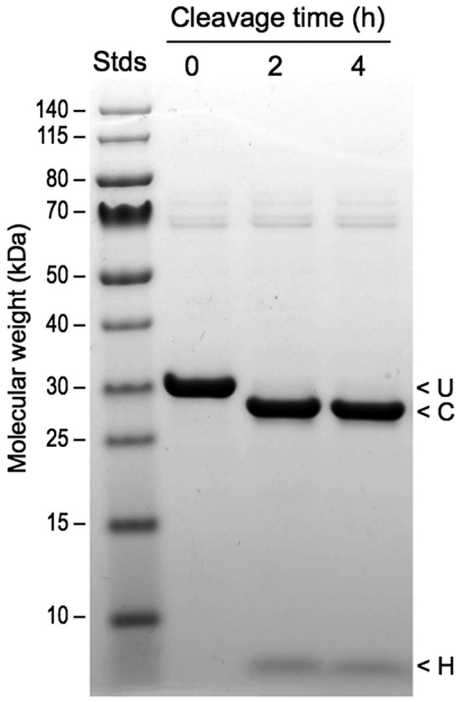

FIGURE 5. **Demonstration of efficient His tag removal.** WT PIMT was incubated for 0, 2, or 4 h with immobilized thrombin as described under "Experimental Procedures." The positions of uncleaved PIMT (*U*), cleaved PIMT (*C*), and free His tag (*H*) are indicated. *Stds*, standards.

dimers. The resistance of these aggregates to heating in SDS-PAGE sample buffer suggests that they are formed either by an unusual covalent cross-link or, more likely, by strong non-covalent interactions of the type seen in β-amyloid, α-synuclein, and numerous other proteins. The results shown in Figs. 3 and 4 tend to rule out intermolecular disulfide bonding or lack of purity as contributors to the high mass bands.

We do not believe that the His/T7 tag plays any role in the small degree of aggregation seen in WT PIMT or in those mutants that have similar low levels of aggregation. This small degree of aggregation was seen previously in PIMT purified from bovine brain (27) and in rat recombinant PIMT expressed with or without the same tags (20, 26). In our experience, aggregation of PIMT is mainly due to its lack of solubility at concentrations above 1.5 mg/ml. It is tempting to speculate that the aggregation prone variants seen here (*e.g.* G175R) are also prone to aggregation *in vivo*, but this is uncertain because of differences in the microenvironment and the presence of the tags.

Enzyme Activity—The results of the activity assays were extremely interesting and highlighted by the complete absence of activity in R36C. Losses of ~40 and 20% were also observed for G175R and F72L, respectively. Equally interesting, and unexpected, is the observation that the two of the variants, A7P and I58V, exhibit methyltransferase activity that is almost double that of the WT. The three-dimensional structure of human PIMT with *S*-adenosyl-L-homocysteine (AdoHcy) bound has been determined to a resolution of 1.6 Å (Protein Data Bank code 1I1N). The guanidino nitrogens of Arg-36 are ~6 Å from the α-carboxyl of the AdoHcy. Given the buried location of this arrangement and its presumed low dielectric environment, a guanidino-carboxyl electrostatic interaction could be critical for positioning AdoMet for its role as the methyl donor. Gly-175 is located on the enzyme surface in the turn of a loop that separates two β-sheet regions of the C-terminal domain. Substitution with an arginine might produce distortion of this region by interactions with the side chains of nearby amino acids such as Gln-198. The phenyl side chain of Phe-72 is exposed to the surface where it might help anchor the two N-terminal helices, a function that could be compromised by the leucine substitution.

Based on the previous studies of human PIMT activity in RBC extracts from genotyped individuals (24, 25), we expected that the specific activity of the common Ile-119 variant (essentially another wild type) would be ~8% higher than WT, but we saw no apparent difference. We suspect the difference seen with the RBC extracts is related to the fact that human RBCs have an average lifetime *in vivo* of ~115 days (29). Any activity loss during this prolonged "*in vivo* incubation" is expected to be greater in the more labile (Val-119) of the two forms. The same explanation has previously been espoused by DeVry and Clarke (25), who also observed higher activity in the Ile-199 variant in human RBC extracts. The *in vivo* incubation effect, in addition to the relative complexity of the extracts, might also explain why preheating at 52 °C for 15 min causes much greater loss of PIMT activity in RBC extracts than it did with our recombinant PIMTs.

The unusual enhancement of enzyme activity seen with A7P and I58V was surprising but might have a simple explanation. Because rare and random mutations typically disrupt protein function, we propose that these mutations decrease the binding affinity of PIMT for AdoHcy (*S*-adenosyl-L-homocysteine), a product of the methylation reaction that competes for AdoMet binding and binds ~20 times stronger (30). A more rapid dissociation of AdoHcy from the active site of these variants could thus increase the turnover rate of the enzyme. Because AdoHcy and AdoMet use the same binding site, these mutations might also worsen AdoMet binding; however, our assays were done at near saturating levels of AdoMet, which would minimize any effects on actual AdoMet binding in the assay. This explanation is supported by the fact that Ile-58 is situated just a few Angstroms from the AdoHcy carboxyl group in the crystallized enzyme (Protein Data Bank code 1I1N). Ala-7 is quite distant from the active site, but substitution with a proline would likely cause a significant change in conformation of the N-terminal region with possible long range effects.

Subsequent to obtaining all the data for this paper, we became aware of several computational algorithms for predicting the effects of non-synonymous SNPs on protein function. Table 2 shows the results for our 14 variants using two distinct but related algorithms: SIFT (Sort Intolerant from Tolerant) and fathmm (functional analysis through hidden Markov models). Both algorithms compare sequences of the subject protein over a range of different organisms to determine the tolerance to variation at the SNP sites being queried. We were impressed with how well both predictions correlated with our experimental activity data. R36C is the only mutation predicted to be damaging by both SIFT and fathmm. G175R was the only other mutation seen as damaging by fathmm but with a less severe

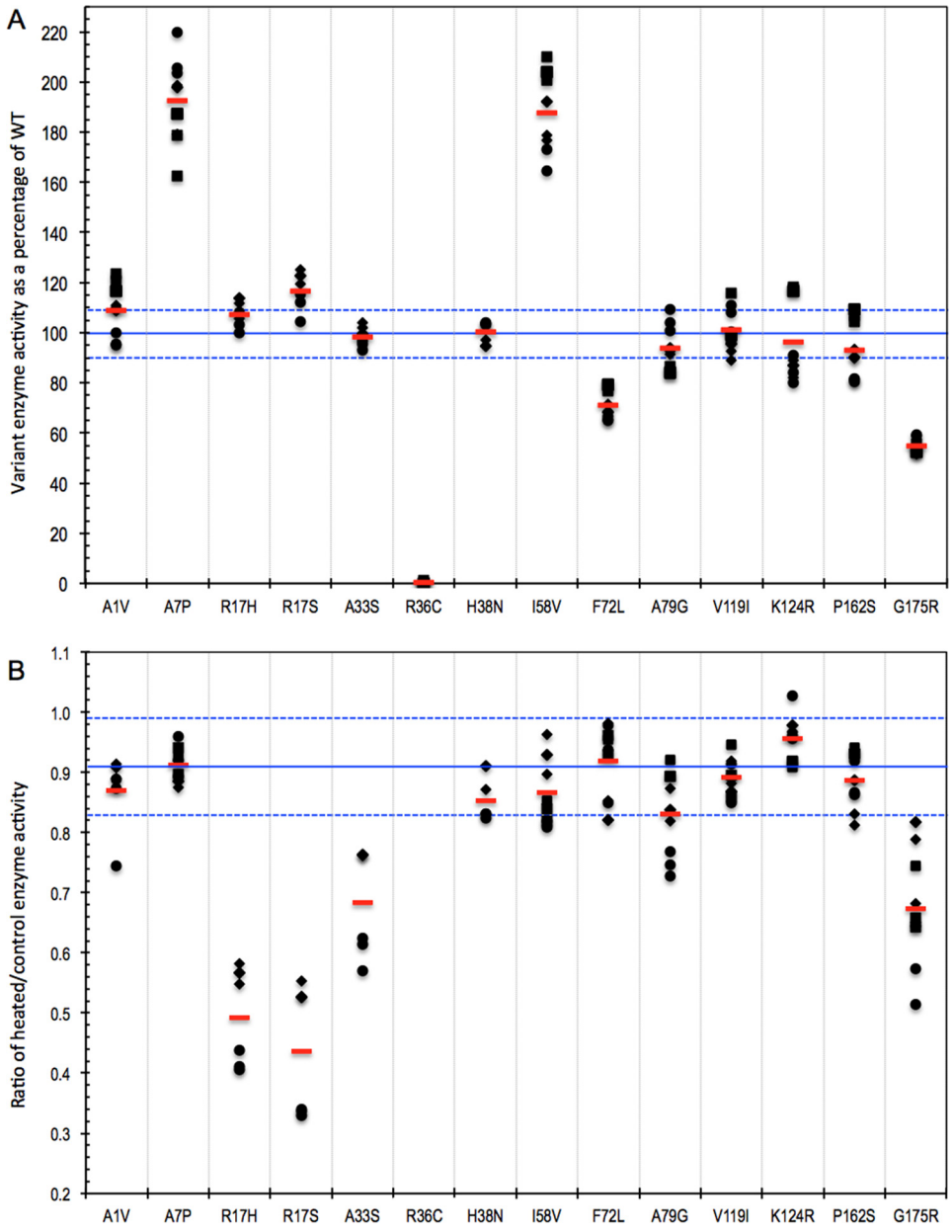

FIGURE 6. **Specific activity and thermal stability of the recombinant human PIMT variants.** *A*, the specific activity of 14 PIMT variants is plotted relative to the activity of the wild type. The methyl-transfer reactions used to generate the data were carried out under initial rate conditions as described under "Experimental Procedures." For a given SNP, two or three experiments were done on a different days and often by a different member of the laboratory. Each symbol (*circle*, *diamond*, or *square*) designates a set of triplicate assays within a given experiment. The *solid horizontal blue line* defines the relative activity of the wild type, to which all the variants are compared. The *blue dashed lines* indicate one standard deviation calculated for 36 sets of triplicate WT assays. The mean of all assays for a given SNP is indicated by a *red bar*. *B*, the thermal stability of all 14 PIMT variants is plotted relative to the activity of the wild type. Plotted here is the activity ratio of heated (15 min at 52 °C)/unheated enzyme. As indicated by the *solid blue line*, WT PIMT retained ~91% of its activity after heating. The *dashed blue lines* indicate two standard deviations of the WT activity ratio gleaned from 36 experiments, each involving triplicate samples of both heated and unheated enzyme.

score than R36C. G175R also had the second lowest SIFT score and barely missed the cutoff for damaging.

A markedly lower thermal stability relative to WT was evident for both mutations at Arg-17. The side chain of Arg-17 thus appears to play an important role in stabilizing the tertiary structure of PIMT. DSF revealed lower T_m values for seven other of the rare PIMT variants (a common finding in rare SNPs) and a higher T_m for the common Ile-119 variant.

As reviewed in the introduction, there is reason to believe, from both mouse and human studies, that a major deficit in human PIMT activity would lead to severe neurological dysfunction in the young and that moderate reductions would contribute to reduced lifespan and quality of life in the aged. As data gleaned from genome-wide association studies continues to grow, studies such as this will help delineate which mutations contribute to disease states at the level of protein function. From the current study, we predict that heterozygosity for R36C, G175R, R17H, or R17S would be detrimental to successful aging, whereas homozygosity (should it ever occur) would produce devastating neuropathology.

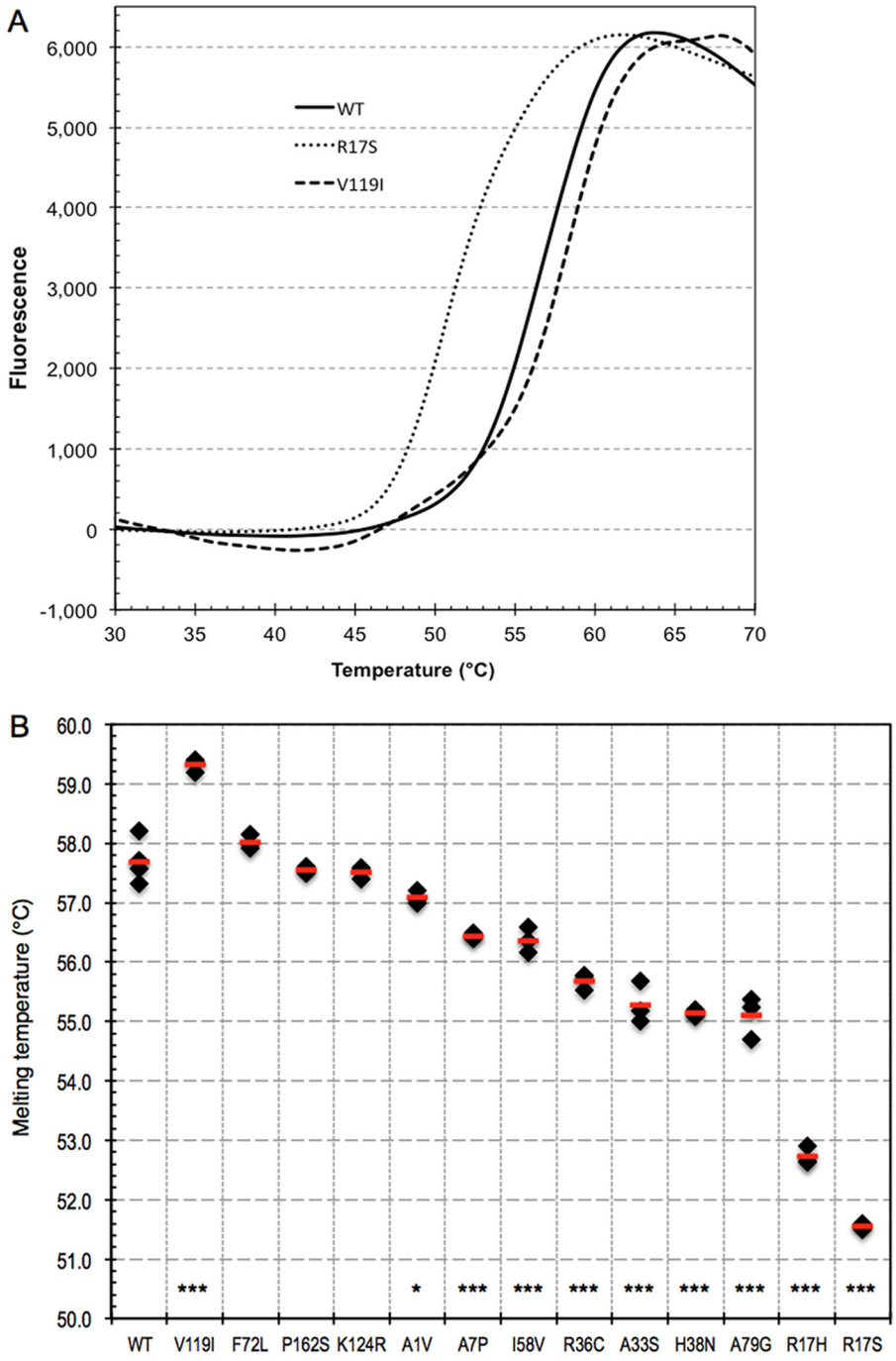

FIGURE 7. **Thermal stability of PIMT variants determined by DSF.** *A*, DSF plots for WT PIMT (Val-119), the other common variant of PIMT (Ile-119), and the most unstable variant (R17S). *B*, summary of T_m values for all PIMT variants in this study, except for G175R, which did not produce a usable T_m curve. *t* test *p* values, for comparisons with WT PIMT, are indicated above each SNP code as follows: *, ≤ 0.05; and ***, ≤ 0.001.

Experimental Procedures

Expression and Purification of PIMT Variants—Custom expression plasmids for all PIMT variants were based on the pET28a(+) vector and were purchased from GenScript (Piscataway, NJ). DNA coding for the human WT PIMT sequence (*pcmt1* gene) was synthesized with codon optimization for expression in *E. coli* and inserted between the BamHI and XhoI sites. Plasmids for SNP variants were generated from the parent WT plasmid using PCR, and the integrity of all plasmid inserts was verified by DNA sequencing.

Expression and purification of PIMT variants was carried out in our laboratory using *E. coli* BL21(DE3) as described previously (20). The purified WT PIMT had a specific activity of ~16,000 pmol/min/mg using γ-globulin as the methyl acceptor (27). Proteins were stored at −80 °C at concentrations ranging from 0.3 to 1.2 mg/ml in buffer consisting of 25 mM Tris-Cl, pH 7.0, 150 mM NaCl, 5 mM 2-mercaptoethanol, and 10% (w/v) glycerol. Protein concentrations were determined in triplicate by a microtiter plate version of the Bradford assay (31) with reagent and protocol from Bio-Rad and bovine serum albumin as the standard.

TABLE 2

Computational predictions for the effects of SNPs on PIMT function

Predictions were calculated using online versions of SIFT (Sort Intolerant From Tolerant) and fathmm (Functional Analysis Through Hidden Markov Models). TOL means tolerated, and DAM means damaging or non-tolerated. Scores of less than 0.05 or −3.00 are considered damaging for SIFT and fathmm, respectively. The two variants that we found to be most damaged (R36C and G175R) are indicated with boldface.

	SIFT		fathmm	
Mutation	**Effect**	**Score**	**Effect**	**Score**
A1V				
A7P	TOL	0.14	TOL	−2.38
R17S	TOL	0.22	TOL	−1.65
R17H	TOL	0.12	TOL	−2.81
A33S	TOL	0.53	TOL	−1.09
R36C	**DAM**	**0.00**	**DAM**	**−9.18**
H38N	TOL	0.32	TOL	−1.96
I58V	TOL	0.31	TOL	−2.91
F72L	TOL	0.37	TOL	+0.38
A79G	TOL	0.33	TOL	−2.22
V119I	TOL	0.36	TOL	+0.04
K124R	TOL	0.31	TOL	−0.96
P162S	TOL	0.37	TOL	−1.42
G175R	**TOL**	**0.06**	**DAM**	**−7.57**

To assess the effect of the His tag on enzyme activity, WT PIMT was treated with immobilized thrombin using the regents and protocol provided with the thrombin CleanCleave™ kit from Sigma. After cleavage, the treated enzyme was dialyzed against PIMT storage buffer, and the protein concentration was redetermined. Complete cleavage in a 2-h incubation was verified by SDS-PAGE. Cleaved and uncleaved versions of WT PIMT were then assayed for activity in the same experiment.

Electrophoresis and Western Blotting—SDS-PAGE was carried out on 1-mm NOVEX NuPAGE 4–12% gels using the MES running buffer (Thermo Fisher). The gels were stained with 0.05% Coomassie Blue R-250. For Western blotting, unstained proteins were transferred to a PVDF membrane (0.45 μm) that was subsequently blocked with 5% nonfat milk and probed with a 1/10,000 dilution of HRP-conjugated goat anti-T7 antibody (Bethyl Labs, Montgomery, TX). Immunostaining as carried out with 3,3′,5,5′-tetramethylbenzidine (TMB) using the 1-Step™ TMB-Blotting Substrate reagent from Thermo Fisher. PageRuler™-prestained protein standards were also from Thermo Fisher.

PIMT Activity Assays—PIMT methyl transferase activity was measured in triplicate samples under initial rate conditions using bovine γ-globulin as the methyl acceptor. Prior to each set of assays, PIMT samples (in reaction buffer plus γ-globulin) were split into two groups. One group was subjected to a preheat at 52 °C for 15 min prior to the assay, whereas the other group remained on ice. Assays were carried out in a final volume of 50 μl containing 1) 100 mM BisTris-Cl (pH 6.4), 2) 5.0 mg/ml bovine γ-globulin (from a stock of 25 mg/ml in 10 mM HCl), 3) 0.05 μg of PIMT, and 4) 10 μM *S*-adenosyl-[*methyl*-^{3}H]L-methionine ([^{3}H]AdoMet, 10,000 dpm/pmol). Components 1–3 were combined and preincubated in a water bath at 30 °C for 2.0 min. The [^{3}H]AdoMet was added, and the reaction was allowed to proceed for 10.0 min, followed by the addition of 750 μl of ice-cold 7% (w/v) trichloroacetic acid to terminate the reaction and precipitate the protein. Pellets were recovered by centrifugation, washed once with 800 μl of water, and then dissolved in 100 μl of 0.2 M NaOH containing 2% (v/v) MeOH. 50 μl of this solution was quickly transferred to folded filter paper lodged in the cap of a 4-dram glass vial prefilled with 2.5 ml of Liquiscint counting fluid, and the vial was then rapidly capped. After incubation at 40 °C for 1 h to allow hydrolysis of the protein methyl esters and transfer of [^{3}H]methanol to the scintillation fluid, the cap was replaced, and the vial was counted by liquid scintillation. The protein values used in the specific activity calculations refer only to the fraction of protein that runs at 28–30 kDa. This was determined by integrating the protein stain in each lane of Fig. 2.

Differential Scanning Fluorimetry—The thermal stability of PIMT variants was determined using an Mx3005P quantitative PCR machine (Agilent Technologies). Each 40-μl sample contained 20 μl of PIMT (0.29–0.58 mg/ml in storage buffer, pH 7.0) and 40 μM Sypro Orange dye. Fluorescence (excitation and emission wavelengths of 492 and 610 nm, respectively) was recorded over the range of 25–95 °C with a temperature gradient of 1 °C/min. All variants were tested in triplicate on the same plate, and all edge wells were avoided. T_m values were extracted as the inflection point of the fluorescence curves.

Calculations and Statistics—Each activity-stability experiment consisted of triplicate samples of WT heated (Wh), WT unheated (Wu), mutant heated (Mh), and mutant unheated (Mu) all assayed in parallel to minimize the effects of potential day to day variation in the specific activity of the [^{3}H]AdoMet (an inherently unstable compound) and water bath temperatures. To calculate the activity of each mutant relative to WT, we calculated, within a given experiment, all nine possible ratios of the individual samples (Wu1/Mu1, Wu1/Mu2 . . . Wu3/Mu3). From these nine ratios we calculated the average and standard deviation. For the preheat stability data, we calculated the average and standard deviation of all nine ratios of heated/unheated for each enzyme tested. For the DSF data, *p* values were obtained using the two-tailed, heteroscedastic *t* test.

Author Contributions—C. J., B. C., J.-L. B., K. N., E. H., M. M., and J. K., conducted the experiments. D. W. A., C. J., and B. C. analyzed the data. D. W. A. conceived and designed the project and wrote the paper.

Acknowledgments—We thank Prof. Tom Poulos for discussions on mutation effects on the three-dimensional structure of PIMT and Prof. Celia Goulding for help in obtaining the DSF data.

References

1. Clarke, S. (2003) Aging as war between chemical and biochemical processes: protein methylation and the recognition of age-damaged proteins for repair. *Ageing Res. Rev.* **2,** 263–285
2. Aswad, D. W., Paranandi, M. V., and Schurter, B. T. (2000) Isoaspartate in peptides and proteins: formation, significance, and analysis. *J. Pharm. Biomed. Anal.* **21,** 1129–1136
3. Desrosiers, R. R., and Fanélus, I. (2011) Damaged proteins bearing L-isoaspartyl residues and aging: a dynamic equilibrium between generation of isomerized forms and repair by PIMT. *Curr. Aging Sci.* **4,** 8–18
4. Johnson, B. A., Langmack, E. L., and Aswad, D. W. (1987) Partial repair of deamidation-damaged calmodulin by protein carboxyl methyltransferase. *J. Biol. Chem.* **262,** 12283–12287
5. Johnson, B. A., Murray, E. D., Jr, Clarke, S., Glass, D. B., and Aswad, D. W. (1987) Protein carboxyl methyltransferase facilitates conversion of atypi-

cal L-isoaspartyl peptides to normal L-aspartyl peptides. *J. Biol. Chem.* **262,** 5622–5629
6. McFadden, P. N., and Clarke, S. (1987) Conversion of isoaspartyl peptides to normal peptides: implications for the cellular repair of damaged proteins. *Proc. Natl. Acad. Sci. U.S.A.* **84,** 2595–2599
7. Brennan, T. V., Anderson, J. W., Jia, Z., Waygood, E. B., and Clarke, S. (1994) Repair of spontaneously deamidated HPr phosphocarrier protein catalyzed by the L-isoaspartate-(D-aspartate) *O*-methyltransferase. *J. Biol. Chem.* **269,** 24586–24595
8. Reissner, K. J., Paranandi, M. V., Luc, T. M., Doyle, H. A., Mamula, M. J., Lowenson, J. D., and Aswad, D. W. (2006) Synapsin I is a major endogenous substrate for protein L-isoaspartyl methyltransferase in mammalian brain. *J. Biol. Chem.* **281,** 8389–8398
9. Dimitrijevic, A., Qin, Z., and Aswad, D. W. (2014) Isoaspartyl formation in creatine kinase B is associated with loss of enzymatic activity; implications for the linkage of isoaspartate accumulation and neurological dysfunction in the PIMT knockout mouse. *PLoS One* **9,** e100622
10. Johnson, B. A., Najbauer, J., and Aswad, D. W. (1993) Accumulation of substrates for protein L-isoaspartyl methyltransferase in adenosine dialdehyde-treated PC12 cells. *J. Biol. Chem.* **268,** 6174–6181
11. Kim, E., Lowenson, J. D., MacLaren, D. C., Clarke, S., and Young, S. G. (1997) Deficiency of a protein-repair enzyme results in the accumulation of altered proteins, retardation of growth, and fatal seizures in mice. *Proc. Natl. Acad. Sci. U.S.A.* **94,** 6132–6137
12. Yamamoto, A., Takagi, H., Kitamura, D., Tatsuoka, H., Nakano, H., Kawano, H., Kuroyanagi, H., Yahagi, Y., Kobayashi, S., Koizumi, K., Sakai, T., Saito, K., Chiba, T., Kawamura, K., Suzuki, K., *et al.* (1998) Deficiency in protein L-isoaspartyl methyltransferase results in a fatal progressive epilepsy. *J. Neurosci.* **18,** 2063–2074
13. Kosugi, S., Furuchi, T., Katane, M., Sekine, M., Shirasawa, T., and Homma, H. (2008) Suppression of protein L-isoaspartyl (D-aspartyl) methyltransferase results in hyperactivation of EGF-stimulated MEK-ERK signaling in cultured mammalian cells. *Biochem. Biophys. Res. Commun.* **371,** 22–27
14. Diliberto, E. J., Jr., and Axelrod, J. (1976) Regional and subcellular distribution of protein carboxymethylase in brain and other tissues. *J. Neurochem.* **26,** 1159–1165
15. Mizobuchi, M., Murao, K., Takeda, R., and Kakimoto, Y. (1994) Tissue-specific expression of isoaspartyl protein carboxyl methyltransferase gene in rat brain and testis. *J. Neurochem.* **62,** 322–328
16. Boivin, D., Bilodeau, D., and Béliveau, R. (1995) Immunochemical characterization of L-isoaspartyl-protein carboxyl methyltransferase from mammalian tissues. *Biochem. J.* **309,** 993–998
17. Qin, Z., Yang, J., Klassen, H. J., and Aswad, D. W. (2014) Isoaspartyl protein damage and repair in mouse retina. *Invest. Ophthalmol. Vis. Sci.* **55,** 1572–1579
18. Ikegaya, Y., Yamada, M., Fukuda, T., Kuroyanagi, H., Shirasawa, T., and Nishiyama, N. (2001) Aberrant synaptic transmission in the hippocampal CA3 region and cognitive deterioration in protein-repair enzyme-deficient mice. *Hippocampus* **11,** 287–298
19. Vitali, R., and Clarke, S. (2004) Improved rotorod performance and hyperactivity in mice deficient in a protein repair methyltransferase. *Behav. Brain Res.* **153,** 129–141
20. Zhu, J. X., Doyle, H. A., Mamula, M. J., and Aswad, D. W. (2006) Protein repair in the brain, proteomic analysis of endogenous substrates for protein L-isoaspartyl methyltransferase in mouse brain. *J. Biol. Chem.* **281,** 33802–33813
21. Qin, Z., Dimitrijevic, A., and Aswad, D. W. (2015) Accelerated protein damage in brains of $PIMT^{+/-}$ mice; a possible model for the variability of cognitive decline in human aging. *Neurobiol. Aging* **36,** 1029–1036
22. Farrar, C. E. (2004) The physiological relevance of protein L-isoaspartyl (D-aspartyl) 0-methyltransferase in the mammalian brain. Ph.D. thesis, University of California, Los Angeles
23. Johnson, B. A., Shirokawa, J. M., Geddes, J. W., Choi, B. H., Kim, R. C., and Aswad, D. W. (1991) Protein L-isoaspartyl methyltransferase in postmortem brains of aged humans. *Neurobiol. Aging* **12,** 19–24
24. David, C. L., Szumlanski, C. L., DeVry, C. G., Park-Hah, J. O., Clarke, S., Weinshilboum, R. M., and Aswad, D. W. (1997) Human erythrocyte protein L-isoaspartyl methyltransferase: heritability of basal activity and genetic polymorphism for thermal stability. *Arch. Biochem. Biophys.* **346,** 277–286
25. DeVry, C. G., and Clarke, S. (1999) Polymorphic forms of the protein L-isoaspartate (D-aspartate) *O*-methyltransferase involved in the repair of age-damaged proteins. *J. Hum. Genet.* **44,** 275–288
26. David, C. L., and Aswad, D. W. (1995) Cloning, expression, and purification of rat brain protein L-isoaspartyl methyltransferase. *Protein Expr. Purif.* **6,** 312–318
27. Aswad, D. W., and Deight, E. A. (1983) Purification and characterization of two distinct isozymes of protein carboxymethylase from bovine brain. *J. Neurochem.* **40,** 1718–1726
28. Huynh, K., and Partch, C. L. (2015) Analysis of protein stability and ligand interactions by thermal shift assay. *Curr. Protoc. Protein Sci.* **79,** 28.9.1-14
29. Franco, R. S. (2012) Measurement of red cell lifespan and aging. *Transfus. Med. Hemother.* **39,** 302–307
30. Johnson, B. A., and Aswad, D. W. (1993) Kinetic properties of bovine brain protein L-isoaspartyl methyltransferase determined using a synthetic isoaspartyl peptide substrate. *Neurochem. Res.* **18,** 87–94
31. Bradford, M. M. (1976) A rapid and sensitive method for the quantitation of microgram quantities of protein utilizing the principle of protein-dye binding. *Anal. Biochem.* **72,** 248–254